

Adsorptive Removal of Oxytetracycline Using Polymer Coated Magnetic Nanoparticulate Activated Carbon: Synthesis, Characterization and Adsorption Isotherms and Kinetics Studies

Uğurlu, Mehmet*+•

Department of Chemistry, Faculty of Science and Art, Ağrı İbrahim Çeçen University, 04000 Ağrı, TURKEY

Osman, Huseyn

Department of Chemistry, Faculty of Science, Muğla Sıtkı Kocman University, 48000 Muğla, TURKEY

Vaizoğulları, Ali İmran

Vocational School Healthcare Med Lab Program Muğla Sıtkı Kocman University, 48000 Muğla, TURKEY

Chaudhary, Abdul Jabbar

Department of Life Sciences, College of Health, Medicine and Life Sciences, Brunel University London, UB8, 3PH, UK

ABSTRACT: In the presented study, the removal of oxytetracycline (OTC) from aqueous solution by adsorption was investigated onto Active Carbon (AC), Magnetic activated carbon (MagAC), Styrene-Butadiene-Styrene Magnetic Activated Carbon (SBS/MagAC) and poly charbon magnetic activated carbon (PC/MagAC). The process optimization was carried out by investigating the effects of pH, temperature, solid-liquid ratio, adsorbent type, and initial concentrations. The data showed that adsorption reached equilibrium in as little as one hour. less adsorption at low pH values and more at approximately 5.0 values. However, all the materials performed well at room temperature when the situation is examined in terms of kinetics. It was also observed that AC, MagAC, and PC/MagAC are more effective than SBS/MagAC and the initial concentration decreased from 100 ppm to 20 ppm with adsorbents. In addition, at lower concentrations, when 25 ppm and 50 ppm were used, it was observed to 2.5 ppm and 5.0 ppm values. The kinetic results presented that the pseudo-second-order model ($r^2 \geq 0.99$) was more effective than that of the pseudo-first-order model ($r^2 < 0.90$). Also, the Intra-particle kinetic model in the adsorption process exhibited two different stages with the diffusion of inter-particle and external diffusion. Adsorption isotherms for all adsorbents were fitted to Langmuir models more effectively than Freundlich models ($r^2 \geq 0.99$). Thermodynamics parameters were also calculated. It is seen that OTC can be removed more easily from the aqueous medium by using magnetic and polymeric materials.

KEYWORDS: Activated carbon; Magnetic adsorbent; Oxytetracycline (OTC); Isotherm; Kinetics.

* To whom correspondence should be addressed.

+ E-mail: mehmetu@mu.edu.tr & mugurlu@agri.edu.tr

• Other Address: Department of Chemistry, Faculty of Science, Muğla Sıtkı Kocman University, 48000 Muğla, TURKEY
1021-9986/2022/9/2986-3006 21/\$7.01

INTRODUCTION

Recently, the use of antibiotics to protect both human and animal health is increasing all over the World. However, this widespread use has become an important issue in terms of public health and environmental pollution problems in recent years [1]. Among them, Oxytetracycline (OTC) has a wide range of uses in the treatment of infections caused by poultry and fish farming [2]. The studies confirm the existence of OTC in different environmental medium such as soil, water systems and sediments in the worldwide [3]. In these environment systems, OTC has adverse effect for the microorganisms' genetic variance resulting in forms of drug-resistant bacteria or pathogens, and pose a risk to the ecosystem and human health. Unfortunately, removing the low concentration of OTC is not possible in the traditional water treatment plants. This situation makes it inevitable that a feasible and effective OTC removal method is urgently established [4-5]. Therefore, removing OTC from the aqueous solution is of great environmental importance. In the literature study, there are many techniques for removing OTC using alumina particles, adsorption on marina sediments, activated sludge, anionic and cationic surfactants, photocatalysis using sepiolite and other adsorption studies [6-10]. Among these, adsorption is an effective and suitable method for developing countries due to low chemicals and materials consumption [11]. In particular, adsorption is most commonly used to remove micro-pollutants, especially hydrophilic compounds such as OTC, in this process the surface charge of the adsorbent material can be easily modified. However, although the selectivity of the adsorption method is not very good, a specific adsorbent can be obtained by surface modification [12]. Modification of the adsorbent gains importance for the efficiency and selectivity of removing contaminants from the environment with natural adsorbents with a small specific surface area is necessary

The most problematic and undesirable situation in the adsorption process is the removal and recovery of nano-based adsorbent materials from the reaction systems. These nano-based materials can be released into the ecosystem and need to be removed for safe disposal. It has been reported that this difficulty can be solved by simply and effectively exposing the reaction system to external magnetic fields. However, this approach can only be used for the separation of magnetic nanoscale materials [13-14].

In literature studies, iron-based magnetic nanopowders are most widely used and preferred as material candidates due to their magnetic and other distinctive properties [15-16].

The application of modified activated carbon, containing iron particles, is the commonly used adsorbent to remove a variety of environmental contaminants from various waste streams. For example, Activated Carbon (AC) containing iron components (FeO , Fe_2O_3 or Fe_3O_4) have been recently used for the treatment of food waste [17], effluent streams containing various organic compounds [18], Cr (VI) [19], antibiotics [20], different heavy metals and As (V) [21]. In addition, AC can also be used for different purposes after processing with certain polymeric materials. In the literature studies, effective mercury removal was carried out using polymer coated activated carbon. In this study, polysulfide-rubber (PSR) polymer, a sulfur-rich compound, was used to increase affinity to remove mercury with activated carbon. Hg-Cl and Hg-S interactions on the activated carbon surface of the chemical bond with mercury have been reported [22].

The previous studies have stated that it is difficult to control an electric or magnetic field since activated carbon powders has not any electrical charge. It can also create secondary contamination after adsorption processes and it should have an electric or magnetic effect for trapping, restoring and recycling to prevent its release into the environment. In the literature study, AC was obtained from rice husk and then modified using magnetic material. The resultant adsorbent material has high surface area ($770 \text{ m}^2/\text{g}$) and 2.78 emu/g saturation magnetization (Ms) with 23% Fe_3O_4 coating. The material has high adsorption capacity and was successfully for the removal of Methylene Blue (MB) [23]. In another study, it has been reported that activated carbon modified using magnetic nanoparticle (AC- Fe_3O_4 MNPs) have additional advantages over the conventional AC materials. These modified AC materials are effective adsorbent materials for the removal of various contaminants such as aniline from both water and wastewater streams [24]. In this study, the synthesis and application of magnetic activated carbon will be investigated due to its high BET surface area, superior adsorbent capacity, and strong interaction with various organic compounds.

We now report on the synthesis, characterization and application of activated carbon modified with magnetic nanoparticles for the removal of OTC from aqueous systems. Firstly, samples of Active Carbon (AC), magnetic

activated carbon (MagAC), styrene-butadiene styrene magnetic activated carbon (SBS/MagAC) and poly carbonate magnetic activated carbon (PC/MagAC) were synthesized and characterized as new adsorbents. In OTC adsorption experiments, temperature, solid-liquid ratio, adsorbent type, initial concentrations and solution pH were investigated by carrying out experiments on a constant shaker. The efficiency of different adsorbents was calculated and compared by investigating adsorption kinetics and thermodynamic parameters.

EXPERIMENTAL SECTION

Preparation of adsorbents

Activated Carbon (AC)

The activated carbon samples used in the study were obtained commercially, Sigma-Aldrich, 242276. Other iron samples were also obtained commercially (ZAG, ZK.100380.1000) and prepared according to literature studies [25].

Magnetic Activated Carbon (MagAC)

FeCl₃ (1.08 g) and FeCl₂ (2.40 g) were added to 150 mL of distilled water and shaken at 60-65 °C for 1 hour. A 5 g of activated carbon was then added to these samples and shaken at the same temperature for 2 hours. In the final step, 5 g of NaOH was added while stirring the mixture for 1 h and aged at overnight. After several washes with distilled water, it was dried to constant weight.

Styrene-Butadiene Styrene Magnetic Activated Carbon (SBS/MagAC)

SBS (1.0g) + THF/DMF 50mL (30:20) samples were prepared and stirred at 60-65 °C for 2 hours. Then 5 g of activated carbon was added to the same temperature for one hour. To this mixture, FeCl₃ (1.08 g) + FeCl₂ (2.40 g) was added and the mixture was stirred at 60-65°C for 2 hours. In the final step, 5 g of NaOH was added to the samples stirred for 1 hour and allowed to stand overnight. These samples were washed several times with distilled water, then filtered and dried to a constant weight in an oven.

Poly Charbonate Magnetic Activated Carbon (PC/MagAC)

PC (1.0 g) and THF/DMF 50 mL (30:20) samples were taken and stirred at 60-65 °C for 2 h. 5g of activated carbon was added and stirred at the same temperature for one hour. FeCl₃ (1.08 g) + FeCl₂ (2.40 g) was then added and the

mixture was stirred for 2 hours at 60-65°C. In the final step, 5 g of NaOH was added and the mixture was stirred for 1h. After washing several times with distilled water, the filtered samples were dried to a constant weight in an oven.

Characterization processes

The characterization of the adsorbents were carried out using Perkin Elmer Lambda 35 UV-Vis Spectrophotometer, Perkin Elmer Pyris 1 for Thermogravimetric Analyzer, Perkin Elmer Diamond for Differential Scanning Calorimeter, Jsm-7600f for Scanning Electron Microscope, Rigaku-Smart-Lab-X-Ray Diffractometer for XRD, Fourier Transform Infrared Spectrophotometer for Thermo Scientific. Nicolet Is10 and Micromeritics TriStar II PLUS for BET analysis.

Physical Characteristics of Oxytetracycline hydrochloride (OTC)

Antibiotics such as (OTC), chlorotetracyclines (CTC) are high quality, widely used and low-cost antibiotics. They are used to treat diseases in livestock, in humans, to prevent a disease or to stimulate growth. Their solubility in aqueous solutions is high and their half-life in the environment is long. The presence of these antibiotics in the environment is dangerous for the ecosystem. Physicochemical properties are given below

Synonyms	5-Hydroxytetracycline hydrochloride (OTC)
Empirical Formula	C ₂₂ H ₂₄ N ₂ O ₉ · HCl
Appearance	Aerosol containing liquefied gas
Color	Blue
Odor	Solvent-like
Flash point	-80 °C
Flammability (solid, gas)	Flammable aerosol
Upper explosive limit / Metaflammability limit	9,5 % (V)
Lower explosive limit / Lower flammability limit	1.8 % (V)
Density	0.92 g/cm ³

Adsorption experiments and oxytetracycline (OTC) determination

The standard stock OTC solution was prepared by dissolving 0.04 g of OTC in 1.0 L distilled water. Adsorption studies were performed using 200 mL of OTC solution containing 50 mg/L. Changes in OTC concentration were determined, before and after the

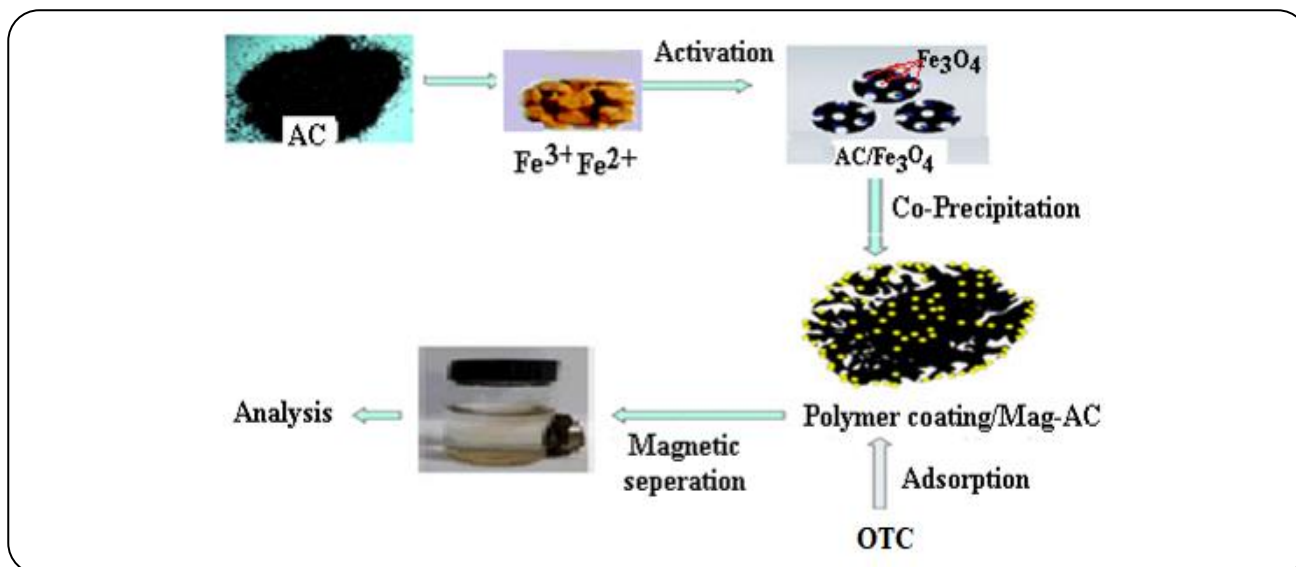


Fig. 1: Synthesis of magnetic materials and general flow chart of experimental design.

adsorption process, with a UV spectrophotometer at 247 nm. All concentrations were determined by using the calibration curve ranging from 20,00–75,00 mg/L. Commercially activated granular Activated Carbon (AC), MagAC, SBS/MagAC and PC/MagAC magnetic adsorbents were used in the experimental study. All adsorption experiments (except experiments examining the pH effect) were carried out at natural pH. Temperature, solid-liquid ratio, adsorbent type, initial concentrations and solution pH were selected as parameters to be investigated for the adsorption studies. In experiments examining the pH effect, the pH of the solution was adjusted using diluted HCl and NaOH solutions and monitored using a pH meter (WTW-Germany. PH 330i). Adsorption experiments were carried out on a constant shaker with a cooling effect. The structure of all synthesized materials, adsorption test apparatus and OTC are shown in Fig. 1, Fig. 2a and Fig. 2b.

Adsorption kinetics

Several kinetic models have been used to determine the adsorption process between pollutant and adsorbent surface. In the present study the pseudo first-order (Eq (1)) and pseudo-second-order (Eq (2)) kinetic models were used [27] and they are given at below respectively [28].

$$\log(q_e - q_t) = \log(q_e) - \frac{k_1}{2.303} t \quad (1)$$

$$\frac{t}{q_t} = \left[\frac{1}{k_2 q_e^2} \right] + \frac{1}{q_e} t \quad (2)$$

Where, q_e is the amount of adsorbed substance (mg/g) per gram of adsorbent at equilibrium, q_t is the amount of adsorbed substance (mg/g) per gram of adsorbent at any instant. The k_1 and k_2 (min^{-1}) are the kinetic rate constants for pseudo and second order kinetic models respectively.

Also, the equation expressing the intra particle diffusion suggested by *Weber and Morris* is given below [29].

$$q_t = k_i t^{1/2} + C \quad (3)$$

Here, c and k_i (in $\text{mg/g min}^{1/2}$) represent the intercept and the intra-particle-diffusion rate constant. The half-time of adsorption $t_{1/2}$ is defined as the time required for adsorption to reach half the equilibrium value. This time is generally used as a measure of the adsorption rate and is calculated with the help of Equation (4).

$$t_{1/2} = \left[\frac{1}{k_2 q_e} \right] \quad (4)$$

Adsorption isotherms

The surface properties and affinity of the adsorbent and their interactions are major reference. Understanding the surface properties and affinity of the adsorbent and its interaction with the adsorbate is extremely important. In this study, adsorption isotherms were carried out under optimized experimental conditions. Physicochemical data were interpreted using both Langmuir and Freundlich isotherm models which Eq.(5) and Eq.(6) below to recognize the adsorption mechanism.

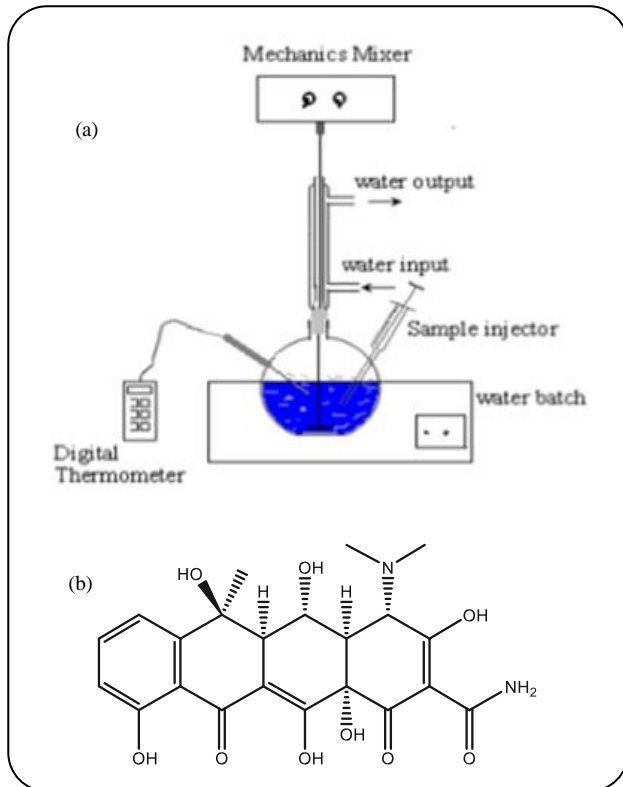


Fig. 2: Adsorption experiment setup (a) and the chemical structure of OTC (b).

Linear state of this equation

$$\frac{C_e}{q_e} = \frac{1}{bQ_0} + \frac{C_e}{Q_0} \quad (5)$$

$$\ln q_e = \ln K_F + \frac{1}{n} \ln C_e \quad (6)$$

the above equations. C_e (in mg/L) is the equilibrium concentration. Q_0 (in mg/g) is the maximum monolayer adsorption capacity. b , K_F and n are respectively called the Langmuir and Freundlich constants.

Adsorption thermodynamics

For the adsorption process, enthalpy, entropy and free energy changes can be determined by the equilibrium constant. These thermodynamic parameters are shown in the following equations (Eq. (7) and Eq. (8))[30].

$$\Delta G^0 = -RT \ln K_e \quad (7)$$

$$\ln K_e = -\frac{\Delta H^0}{RT} + \frac{\Delta S^0}{R} \quad (8)$$

Here, ΔG^0 standard Gibbs free energy. ΔH^0 standard enthalpy and ΔS^0 standard entropy. ΔH^0 and ΔS^0 are

calculated from the slope of the graph of $1/T$ versus $\ln K_e$ and the cut-off point, respectively. Adsorption equilibrium constant can be calculated using the following equation.

$$K_e = \frac{C_{ads}}{C_e} \quad (9)$$

Here, C_{ads} is the concentration (mg/L) of the adsorbed substance at equilibrium and C_e is the concentration of the substance remaining in solution at equilibrium (mg/L).

DISCUSSION AND CONCLUSION

Evaluation of The Findings and The Characterization of Synthesized Materials

All adsorbent materials (AC, MagAC, SBS/MagAC and PC/MagAC) were characterized using various analytical techniques, for example, FT-IR, SEM, EDS, XRD, TGA, DSC and BET. All the related evaluations and comparisons for different adsorbent materials are given in the following subsections.

SEM/EDS images and BET analysis

The morphological structure of adsorbents can give specific information about the adhesion characteristics and mechanism. SEM and EDS results of adsorbents are given in Fig. 3. When the SEM images of the activated carbon are examined, a distinct porous structure is seen, with many cavities, and its outer surfaces are recessed and protruding. In MagAC and PC/MagAC materials, it is seen that the iron and polymers species attach to the porous surface of the activated carbon and the particles inside. SEM image of SBS/MagAC material shows a clearer appearance than the other samples in which a significant change is observed. This is thought to be the result from the interaction of polymers with the pores of the activated carbon (Fig. 3).

In order to obtain the information about the element structure of adsorbent materials, EDS analysis was performed from SEM image. As shown in the EDS graph given in Fig. 3, it is seen that Ca, Fe, C, and O elements are present predominantly on the surface of the adsorbents except activated carbon and with small amounts of Na and Mg elements. Trace amounts of Cu and Si elements are also partially observed in SBS/MagAC material. In addition, when the EDS analysis was examined the highest amount of Ca and C elements were found in these samples. In addition, activated carbon samples obtained by using various polymeric materials and surface and pore size changes are given in Table 1.

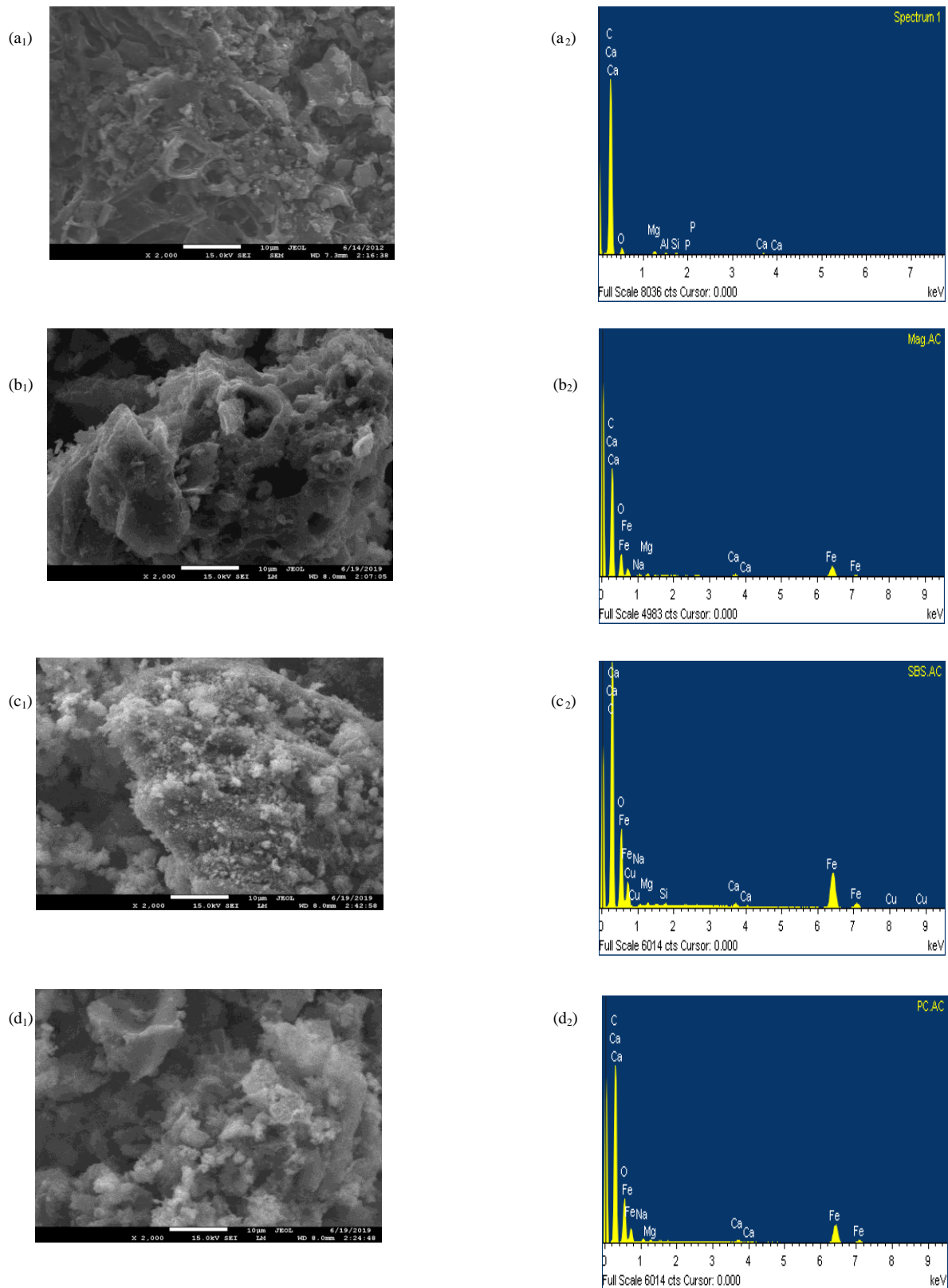


Fig. 3: SEM and EDS images of adsorbent materials a) AC, b) MagAC, c) SBS/MagAC, d) PC/MagAC.

Table 1: Changes in surface and pore size by loading magnetic and polymeric materials on the surface of activated carbon.

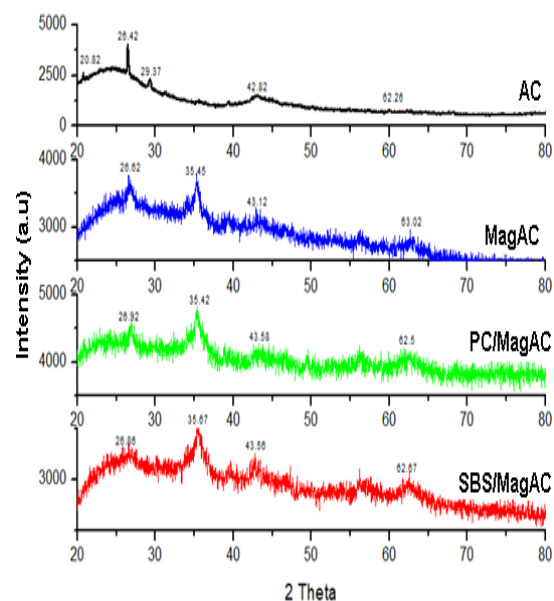
Surface and Pore Parameters	AC	MagAC	SBS/MagAC	PC/MagAC
Surface areas (m ² /g)				
Single point surface area	695.459	642.54	248.49	301.18
BET Surface Area	687.751	636.86	251.31	304.56
Langmuir Surface Area	912.379	845.74	339.63	412.56
t-Plot Micropore Area	395.999	354.35	82.66	89.38
t-plot Surface Area	291.751	291.51	168.65	215.18
Pore volume (cm ³ /g)				
Total pore volume from a single point	0.571	0.598	0.285	0.328
t-Plot micropore volume	0.181	0.157	0.036	0.039
BJH Adsorption cumulative pore volume	0.339	0.396	0.221	0.261
BJH Desorption cumulative pore volume	0.376	0.432	0.234	0.280
Pore size (nm)				
Adsorption average pore width (4V/A with BET)	3.323	3.759	4.551	4.311
BJH Adsorption average pore diameter (4V/A)	7.137	8.020	8.122	8.221
BJH Desorption mean pore diameter (4V/A)	5.472	6.163	6.081	6.191

As can be seen in Table 1, considering the surface area of AC and synthesized materials, it is observed that all surface area parameters follow as AC>MagAC>PC/MagAC>SBS/MagAC. A similar situation is observed when pore volume is examined. When the pore size data are evaluated, the opposite situation is observed. This is attributed to the polymer material reaching and penetrating into the interior of the pores.

XRD images

XRD analysis of magnetic materials obtained with various polymeric materials using activated carbon samples are given in Fig. 4.

Fig. 4 shows the XRD spectra of activated carbon and activated carbon-based catalysis samples. When XRD spectra of pure activated carbon are examined, the characteristic 2 theta degree with 20.82°, 26.42°, 29.37°, 42.82° and 62.26° are seen with sharp peaks. This shows that AC has a regular crystal structure. The diffraction peaks at 26.42 and 42.82 shows (002) and (100) planes respectively. The highest peak intensity was observed at 26.42°. This shows that AC grows in the direction of the surface (002) [31]. In addition, when compared with other synthesized samples, significant decreases in peak

**Fig. 4: XRD images of different adsorbent materials.**

intensity are observed. This shows that AC samples with partially crystalline structure tend to turn into amorphous structure over time. In other words, the diffraction peaks in the other samples except AC were slightly wider. The decrease in the sharp peak intensities of AC indicates

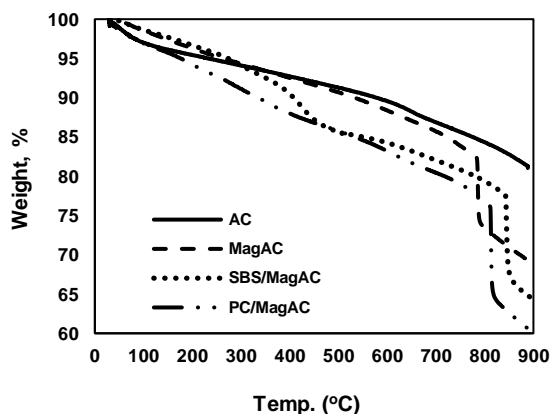


Fig. 5: TGA results of AC, MagAC, SBS/MagAC, and PC/MagAC adsorbents.

that the composite components shift to a little more amorphous structure and also indicates that the particle size decreases to some extent [32].

When the diffraction peaks of the MagAC sample with magnetic content were examined, a diffraction peak at 35.45° which iron components was observed besides the characteristic activated carbon peaks. In all synthesized samples except activated carbon, it is observed that iron peaks are formed as a result of treatment with strong base to ensure complete precipitation of iron ions. The angle of about 35° is seen in each sample. This shows that there is no change in the crystal structure of the PC and SBS used on the Iron components. When we look at SBS/MagAC sample, it is seen that as Full Width at Half Maximum (FWHM) value increases the peak intensity of main diffraction peak decreases. This suggests that SBS provides an effective dispersion on AC. This result shows that the particles of polymeric properties are synthesized with high efficiency of activated carbon samples and that an active dispersion of other magnetic and polymeric components on AC surface is provided.

TGA analysis

The relationship between temperature and mass loss was investigated by using TGA analysis of magnetic materials obtained with various polymeric materials using activated carbon samples and is given in Fig. 5.

In short, TGA is a method used to examine the ability of a substance to maintain its mass (thermal stability) under various conditions. In other words, it is the continuous monitoring of the changes in the mass of the

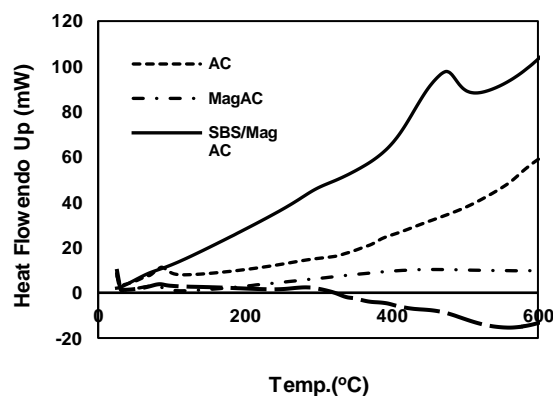


Fig. 6: DSC results of AC, MagAC, SBS/MagAC and PC/MagAC adsorbents.

substance depending on the temperature and evaluating this as a function of the temperature. The data in Fig. 5 show that the TGA values of AC generally lose mass with increasing temperature and a significant peak change occurs. Here, a significant peak change was observed at MagAC and PC/MagAC samples at approximately 800°C and at the other SBS/MagAC samples at 850°C . This shows that the thermogravimetric method is dynamic that the system will never reach equilibrium and that changes in the amorphous and crystalline structure can occur with increasing temperature [33]. In addition, starting from 800°C , mass loss was evident and sharp in all adsorbents. This is particularly related to the decomposition and change of the carbon skeleton found in polymer-coated materials [34].

DSC analysis

DSC analysis results of magnetic materials obtained with various polymeric materials by using activated carbon samples are given in Fig. 6.

The most important applications of thermogravimetric methods are for polymers. The decomposition mechanisms of various polymeric materials can be explained by the information obtained from thermograms. In addition, the investigation behavior characteristic of each type polymer is used in the identification of polymers. In the DSC process, the temperature of the sample and reference is increased at a regular rate by measuring the amount of energy absorbed or released while the sample is heated and cooled or maintained at a constant temperature.

Endothermic heat goes into the sample. Exothermic heat flows out of the sample. The heat lost or recovered as a result of endothermic or exothermic reactions in the sample is recovered. Furthermore, the heating rate is recorded as a function of the sample temperature. When examined in Fig. 6 it is seen that there are endothermic peaks around 100°C in AC samples. In MagAC sample, it is observed that one exothermic peak is formed and it is increased affected by temperature. Exothermic peaks at 500°C in SBS/MagAC samples exothermic peaks at 100°C and 300°C and endothermic peaks at PC/MagAC samples. In addition, it is seen that all the samples of temperature resistance are generally lower [34].

FT-IR images

FT-IR spectra of polymeric coated magnetic materials using activated carbon samples are given in Fig. 7.

a) When the FT-IR spectra of pure activated carbon were examined, it was observed that the peak of -OH group observed at 3041.85 cm^{-1} shifted to 3013.96 cm^{-1} as a result of the interaction with Fe_3O_4 nanoparticles. Therefore, we can infer that adsorption occurs by physical interaction with OH groups on the surface. However, the C-O single bond to which the -OH group is bound and observed at 1216.36 cm^{-1} has been strengthened by the weakening of the -OH group and shifted to 1223.16 cm^{-1} . This is another proof of the interaction of nanoparticles with this group. The peaks of the -CH group observed at 2880.90 cm^{-1} of activated carbon in the free state were significant in the peaks of the C = O group observed at 1714.43 cm^{-1} and the C = C tensile peaks at 1536.03 cm^{-1} . the absence of a change indicates that there was no interaction with these groups.

b) When the FTIR spectrum of the product obtained by the interaction of activated carbon coated with Fe_3O_4 nanoparticles with polycarbonate polymer, the -OH peak observed at 3019.96 cm^{-1} shifted to 3421.76 cm^{-1} . This is due to the hydrogen bond between the -COO group and the -OH molecules in the structure during the bonding of polycarbonate to the MagAC composite material. Another proof of this is the C=O bond peak observed at 1648.86 cm^{-1} in polycarbonate bonded MagAC composite material. This peak was weakened by hydrogen bond formation and appeared at 1648.86 cm^{-1} . Fe-C bonds not observed in MagAC composite material were observed at 603.39 cm^{-1} in polycarbonate bonded MagAC composite material

which explains the bond formed between the surface-coated Fe metal and polycarbonate polymer. C-O bond observed at 1223.16 cm^{-1} in MagAC composite material weakened during the interaction between polycarbonate and MagAC composite material and appeared at 1171.22 cm^{-1} .

c) When the FTIR spectrum of the product obtained by the interaction of Fe_3O_4 coated activated carbon with SBS polymer, no change was observed in the spectrum [35-36].

Adsorption results

Magnetic and polymer coated adsorbents were synthesized on the basis of AC-based material. Solid-liquid ratio, initial concentration, suspension pH and temperature effect were investigated. The variation of the adsorbed amount per gram weight of adsorbents over time was evaluated separately for each parameter.

Effect of solid-liquid ratio

Fig. 8 shows the effect of solid/liquid ratio for the removal yield of OTC using adsorbent materials. As known, the total surface area of the attachment sites is directly proportional to the amount of adsorbent [37]. As seen from the Fig. 8, the removal efficiency of OTC increases with the adsorbent dosage directly.

However, due to the increase in all solid-liquid ratios, there is a significant reduction in the amount of adsorbed, while the amount of adsorbed per gram decreases as the amount of adsorbent increases. This situation is thought to arise from the interaction of the magnetic material in the solution and the properties on the adsorbent surface. In addition, although the adsorption performance is high at low concentration, low removal at the end point, the higher the adsorption rate per gram, the higher the amount of adsorbed substance per gram. The best results in terms of performance are seen in AC, SBS/MagAC, PC/MagAC and MagAC examples, respectively. In addition, since 1.0g/L adsorbent provided a significant increase in removal, subsequent experiments were conducted taking this solid-liquid ratio into account.

Table 2 shows the adsorption capacities for OTC using different types of adsorbents reported in the literature. As can be seen here, different adsorption capacities are seen with different adsorbents. This shows that the adsorption capacity of the magnetic compounds used in the study is high. It seems to be higher than those stated in the literature.

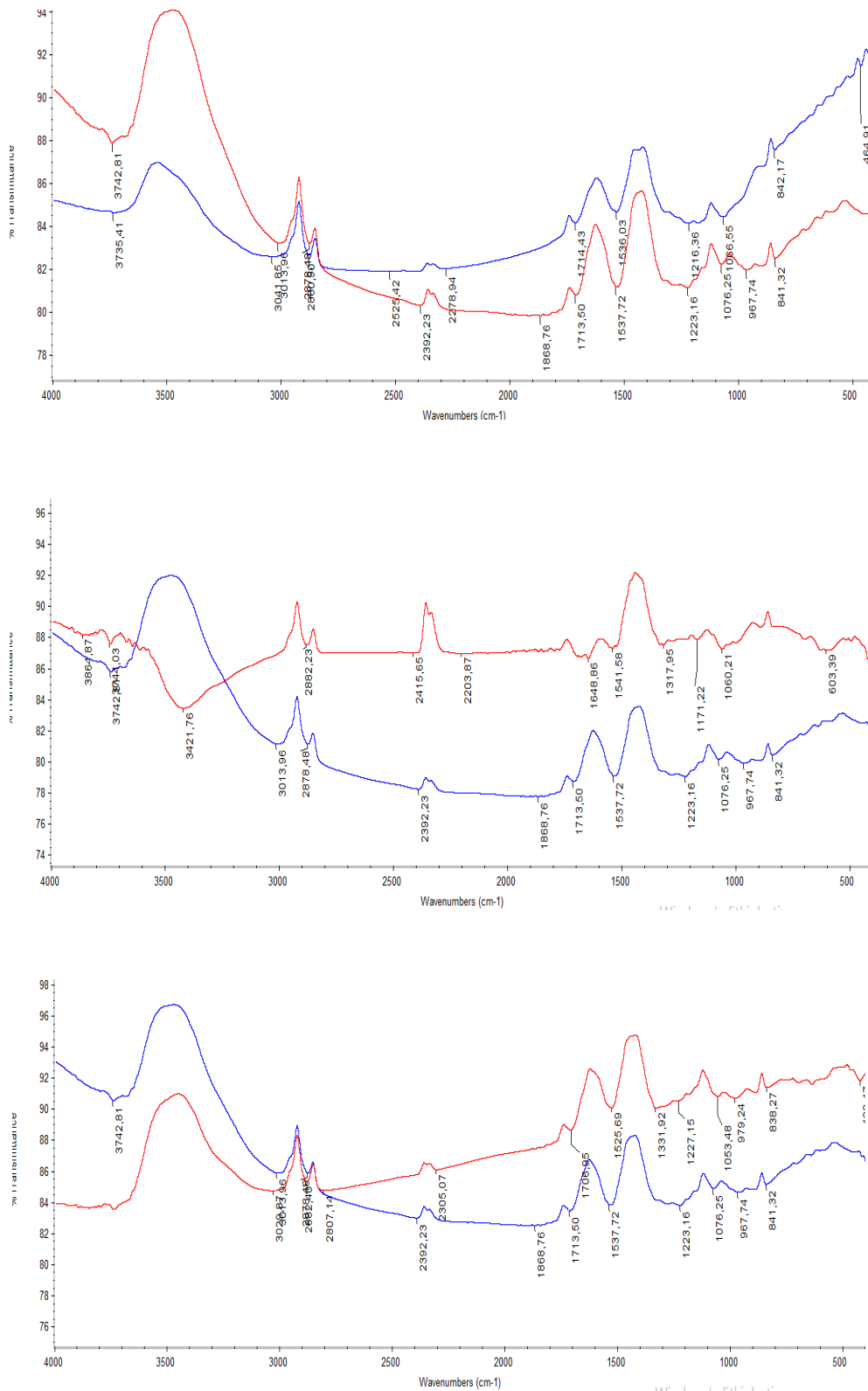


Fig 7: FT-IR results a) AC vs MagAC, b) AC vs PC/MagAC, c) AC vs SBS/MagAC adsorbents.

Table 2: Literature results of the adsorption of OTC by different adsorbents.

Adsorbent	Efficiency of adsorbent at optimum condition (mg/g)	Reference
Graphene oxide magnetic nanoparticycles	45,00	[38]
Maize-straw-derivedbiochar	1,67	[39]
Activated sludge	35.00	[40]
Bomboo charcoal	23.05	[41]
Modified polyacrylamide based cryogels	54.00	[42]
MnAl-Hydroxide	23,10	[43]
Magnetic atapulgite-biochar composite	33.31	[44]
Modify natural sepiolite (SEP)	22.23	[45]
Type of organic sepiolite (C-S-SEP)	43.22	[45]
Activated carbon	60.21	This work
MagAC	62.01	This work
SBS/ MagAC	30.28	This work
PC/ MagAC	58.14	This work

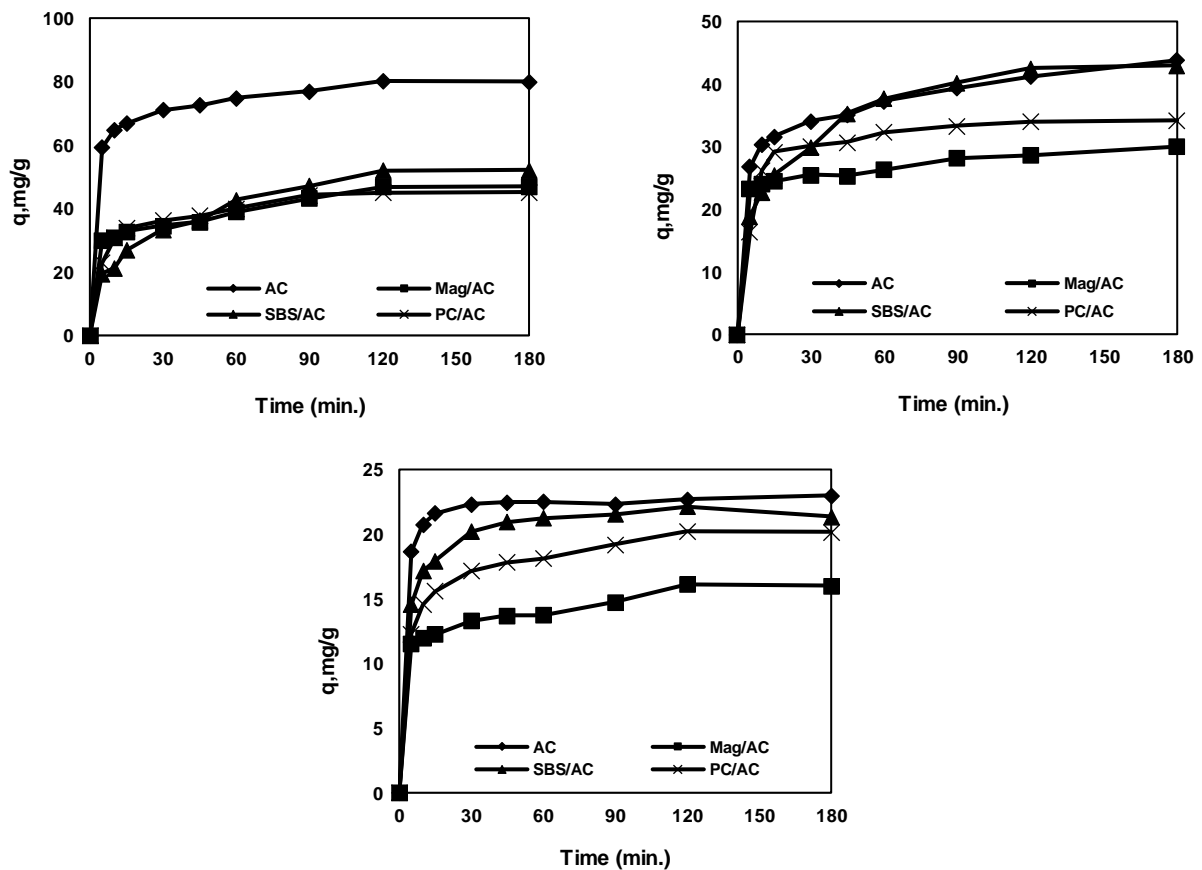


Fig. 8: The amount of OTC adsorbed over time in adsorption with different adsorbents 0.5g/L (a) 1.0 g/L (b), 2.0g/L (c) (298K, natural pH, constant mixing speed, 50ppm).

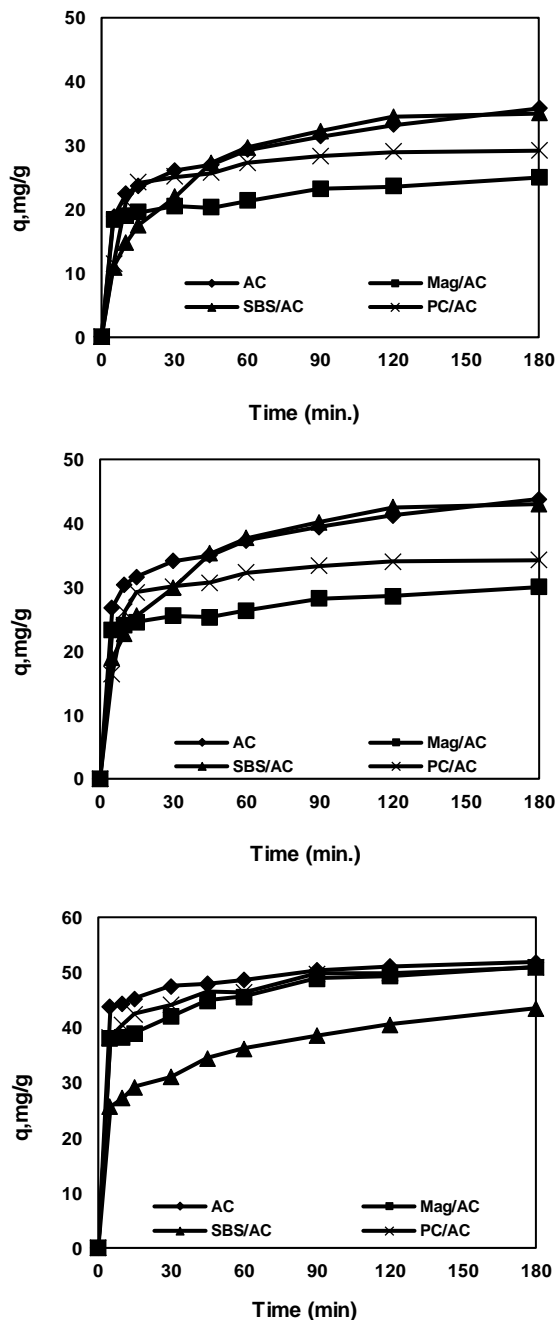


Fig. 9: The amount of OTC adsorbed over time at different temperatures (291 K (a), 298 K (b), 308 K (c) (1.0 g / L, natural pH, constant mixing speed, 50ppm)).

Temperature effect

One of the significant parameters in the adsorption is the temperature which affecting the adsorption medium. Hence it was studied, in three different temperature of 291 K, 298 K, 308 K. The removal efficiency of OTC using adsorbent materials are showed in Fig. 9.

When the temperature effect is examined, it is seen that the efficiency is generally high at room temperature. In addition, it is seen that PC/MagAC and AC samples provide better adsorption with increasing temperature compared to other adsorbents. Here, SBS/MagAC samples appear to be affected by temperature changes. Another observed situation is that adsorption at high temperatures reaches equilibrium in a very short time. In addition, temperature affects the adsorption capacity. In this study, it was observed that the adsorption capacity increased with the increase of temperature and the highest value was at 303 K indicating the endothermic adsorption of OTC onto all adsorbents. There are similar studies supporting this result [46-48].

The Effect of initial concentration

To examine the initial concentration effect, changes in the amount of OTC adsorbed per gram using adsorbent materials are plotted in Fig. 10.

Depending on the changes in the initial concentration, changes in the OTC adsorption capacity of all adsorbents were observed. It was observed that the OTC going efficiency increased with increasing concentration (Fig. 10). This is related to the saturation of the binding sites present as the concentration increases. It is also seen that adsorbents behave differently here. This shows that in all adsorbents has not adequate active adsorption sites to adsorbate the pollutant. It is observed that the adsorption is low in SBS/MagAC samples in low and high concentrations, whereas in other concentrations SBS/MagAC and AC yields better efficiency general, except for SBS/MagAC other samples show similar trends. In addition, the adsorption reaching equilibrium in a short time can be associated with the physical character of the interaction [49].

The effect of pH

In order to investigate the effect of pH. the changes that occur due to suspension pH in OTC adsorption using AC and synthesized magnetic adsorbents are given in Fig. 11.

Considering that OTC has multiple groups such as phenol, amino, and alcohol capable of charged and/or electronic connection, it can be said to have an amphoteric structure [50-52]. The emergence or display of different ionic forms in OTC, depending on the pH values of the solution medium, plays an important role here. In general,

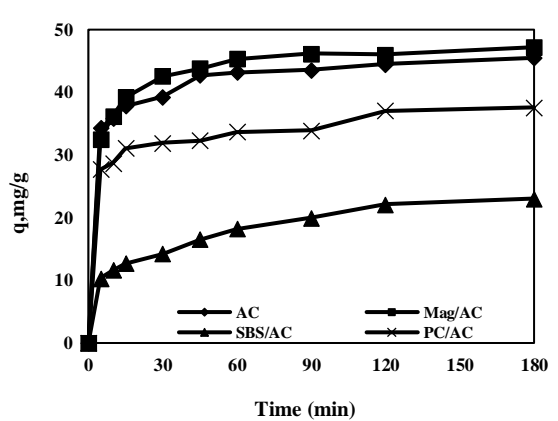
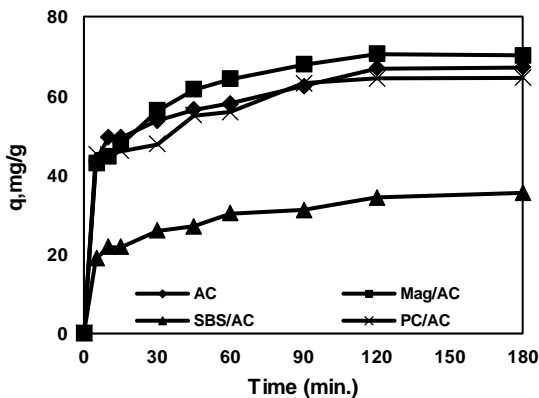
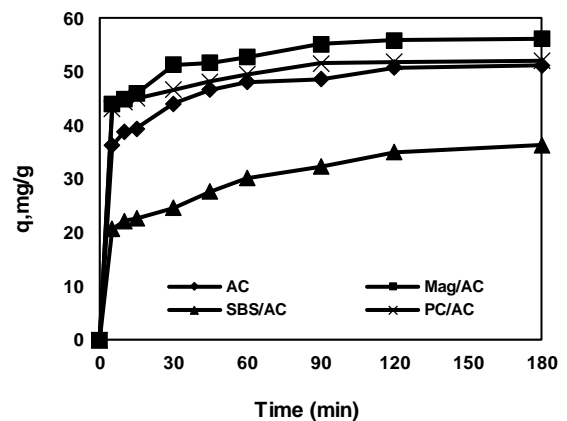
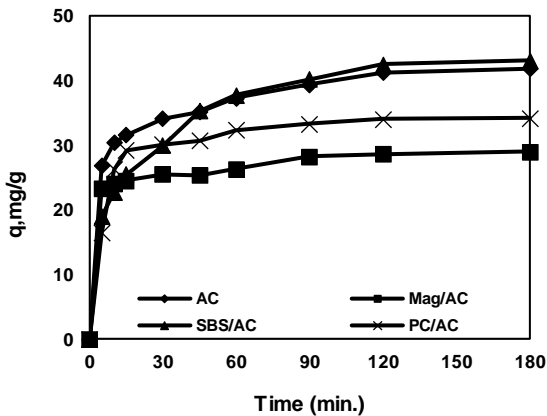
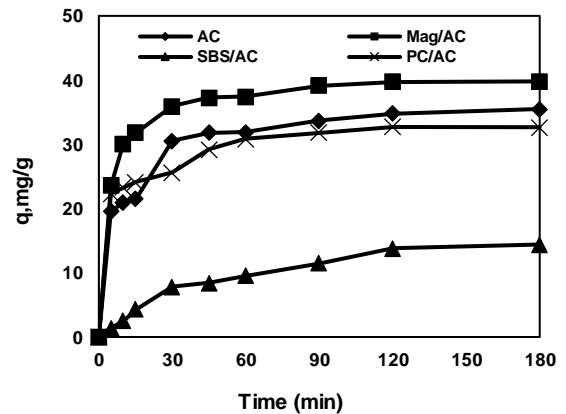
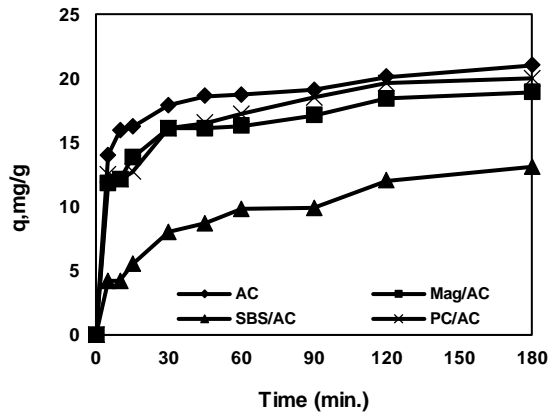


Fig. 10: The amount of OTC adsorbed over time in adsorption at different concentrations 25ppm (a), 50ppm (b), 100ppm (c) (1.0 g/L, 298 K, natural pH, constant mixing speed).

Fig. 11: The amount of OTC adsorbed per gram of adsorbent depending on the pH effect pH:3.0 (a), pH:5.0 (b), pH:7.0 (c), pH 9 (d), mass fraction OTC (e) (1.0 g/L, 298K, 50ppm, constant mixing speed).

there are four different types of OTC at various pH values, such as positive form, neutral form, one negative valence, and two negative valences [53].

The cationic form of OTC⁺⁰⁰ is primarily present at pH below 3.3. the Zwitterion (+ -0) is its main form at pH

between 3.3 and 7.3, and as the pH increases, it turns into deprotonation types (+ - -) (Fig. 11e). When the solution pH is below 5.5, the dominant forms of OTC are OTC⁺⁰⁰ and OTC⁺⁰. Increasing solution pH is thought to increase the negative charge density of all adsorbents, thus increasing

Table 3: Freundlich and Langmuire values for AC, Mag AC, SBS/MagAC and PC/Mag AC.

Adsorbents	Freundlich			Langmuire		
	n	K_f	R^2	$bx10^{-2}$	Q_0	R^2
AC	1,920	12,43	0,83	9,67	91,27	0,99
MagAC	1,287	3,78	0,90	9,37	47,39	1,00
SBS/MagAC	1,982	6,11	0,89	4,18	48,78	0,98
PC/MagAC	1,497	6,55	0,90	3,01	136,98	0,99

the electrostatic attraction between OTC^{+00} or OTC^{+0} and the positively or negatively charged adsorbent surface. This will increase the binding of OTC to adsorbents. However, the dominant types of OTC were OTC^+ and OTC^0 when pH was above 5.5. Increasing solution pH will increase electrostatic repulsion between OTC^+ or OTC^0 and surface charges as this will result in more negative charges on all adsorbents. Therefore, it will reduce the adsorption of OTC to adsorbents, which is consistent with similar studies in the literature [54].

When the pH effect is examined for all adsorbents, the maximum adsorption rates are observed in AC, Mag/AC, PC/MagAC and SBS/MagAC samples, respectively. In addition, it was observed that there was less adsorption at low pH values and more at approximately 5.0 values. This situation can be explained from the anionic and cationic and neutral properties of the surface, as stated in similar studies [55]. The reason for the changes in the solution pH before and after the adsorption is one of the reduction of OTC concentration and ion exchange mechanisms. Because the antibiotic/water environment (weakly acidic) showed better results in OTC adsorption.

Adsorption isotherms

To explain the interaction between OTC and adsorbent, adsorption isotherms which have an important characterization were studied [56]. For this, the most important isotherm models were used to reveal the adsorption behavior of OTC onto adsorbents. The Langmuir adsorption model is an ideal approach due to the uniform use of adsorption areas, the monolayer surface and the absence of material transition on the surface plane [57]. Freundlich isotherm model is based on the assumption that there is multilayer adsorption and an interaction between molecules comparing the Langmuir [58]. When Table 3 is examined, it can be said that the adsorption isotherm model of OTC at all temperatures is attributed to the Langmuir

model ($R^2=0.98$) and the existence of a single layer adsorption [59]. Thus, comparison of the R^2 values for both models (Table 3) showed that adsorption of the mixed pollution by all adsorbents were more consistent with the Langmuir adsorption model. This indicated that monolayer adsorption of OTC on to the surface of adsorbents were significant and most likely the dominant mechanism [59].

Adsorption kinetics

The first order, second order and intraparticle diffusion kinetic results are shown in Table 4a and b. as seen from the Table, OTC adsorption followed the pseudo-second order kinetic model ($R^2=0.99$). also, the adsorption capacity (q_e) is more close to the experimental results indicating the chemical adsorption process (q_e, exp) [54]. The strong electrostatic interaction or ion exchange on the surface for OTC adsorption is consisted with sorption mechanisms which defined chemisorption process [60]. When the initial concentration of the OTC solution changes from 25 mL to 100 mL, it is clear from the adsorption reaction rate values (k_2) that it is different for each adsorbent. (Tables 4a and 4b). Two dominant factors have been proposed: (i) The increase in the initial OTC concentration can be considered as a driving force of the concentration between the adsorbent and the adsorbent in the solution, resulting in further OTC adsorption and (ii) higher concentrations of adsorbate molecules were greater for the active regions [61]. In addition, the appropriateness of the particle diffusion model was examined in the presented study. Here, R^2 value was observed to be significant. Considering the intra-particle diffusion model, the proximity between the experimental and theoretical q_e values shows that all adsorbents are applicable for phenol adsorption, and as a result, surface adsorption and intra-particle diffusion occur simultaneously. This can be attributed primarily to the outer surface of the adsorbents in two stages, and then one by diffusion into the pores [62].

Table 4a: In OTC adsorption of AC and Mag AC and I. II. degree kinetic model and particle diffusion data

Parameters	AC									MagAC								
	First-order	Pseudo-second-order			Intra-particle diffusion					First-order	Pseudo-second-order			Intra-particle diffusion				
	R ²	q _{e(cal)} (mg/g)	q _{e(exp)} (mg/g)	k ₂ (g/mgmin)	R ²	k ₁ (g/mgmin)	C	R ²	t _{1/2} (min)	R ²	q _{e(cal)} (mg/g)	q _{e(exp)} (mgg ⁻¹)	k ₂ (g/mgmin)	R ²	k ₁ (g/mgmin)	C	R ²	t _{1/2} (min)
Ads. dos. (g/L)																		
0,5	0,97	81,30	80,00	0,003	0,99	1,80	59,16	0,90	4,17	0,95	49,01	47,00	0,002	0,99	1,71	25,81	0,96	10,64
1,0	0,98	44,44	43,80	0,002	0,99	1,43	25,47	0,97	11,42	0,97	30,21	30,00	0,006	0,99	0,60	21,99	0,98	5,56
2,0	0,89	23,04	23,00	0,032	0,99	0,28	19,84	0,64	1,36	0,96	16,39	16,00	0,01	0,99	0,43	10,67	0,96	6,25
Temp. (K)																		
291	0,97	43,29	42,90	0,003	0,99	0,76	35,52	0,96	7,77	0,98	41,84	40,40	0,002	0,99	1,72	18,61	0,98	12,38
298	0,98	44,44	43,80	0,002	0,99	1,43	25,45	0,97	11,42	0,98	30,21	30,00	0,006	0,99	0,59	21,99	0,97	5,56
308	0,99	45,24	44,90	0,007	0,99	1,21	27,23	0,96	3,18	0,97	44,84	44,00	0,003	0,99	1,30	27,96	0,96	7,58
Initial Con.(mg/L)																		
25	0,95	21,18	21,00	0,009	0,99	2,12	41,52	0,96	5,29	0,95	19,30	18,90	0,007	0,99	0,63	11,17	0,90	7,56
50	0,98	42,91	41,80	0,003	0,99	1,32	26,05	0,94	7,97	0,96	29,41	29,00	0,008	0,99	0,54	22,27	0,95	4,31
100	0,98	68,96	67,12	0,002	0,99	0,56	14,01	0,91	7,45	0,99	72,99	70,14	0,002	0,99	2,67	39,06	0,91	7,13
Initial pH																		
3,0	0,97	41,66	40,50	0,004	0,99	1,54	23,09	0,83	6,17	0,96	45,66	44,8	0,006	0,99	1,37	25,18	0,88	3,72
5,0	0,99	42,19	41,16	0,004	0,99	1,25	31,14	0,75	6,07	0,97	47,16	46,10	0,005	0,99	1,19	32,40	0,89	4,34
7,0	0,97	44,05	43,50	0,006	0,99	1,22	4,63	0,95	3,83	0,97	45,87	45,20	0,006	0,99	1,52	7,21	0,98	3,69
9,0	0,97	38,31	37,21	0,003	0,99	1,06	25,59	0,89	8,96	0,95	41,49	40,10	0,002	0,99	0,88	31,82	0,93	12,47

Table 4b: In OTC adsorption of SBS/MagAC and PC/MagAC and I. II. degree kinetic model and particle diffusion data.

Parameters	AC									MagAC								
	First-order	Pseudo-second-order			Intra-particle diffusion					First-order	Pseudo-second-order			Intra-particle diffusion				
	R ²	q _{e(calcd)} (mg/g)	q _{e(exp)} (mg/g)	k ₂ (g/mgmin)	R ²	k ₁ (g/mgmin)	C	R ²	t _{1/2} (min)	R ²	q _{e(calcd)} (mg/g)	q _{e(exp)} (mgg ⁻¹)	k ₂ (g/mgmin)	R ²	k ₁ (g/mgmin)	C	R ²	t _{1/2} (min)
Ads. dos. (g/L)																		
0,5	0,98	54,47	52,20	0,001	0,99	3,25	13,97	0,95	19,16	0,91	46,92	45,20	0,003	0,99	1,82	24,6	0,86	7,37
1,0	0,99	45,66	43,00	0,002	0,99	2,27	16,92	0,91	11,63	0,95	35,08	34,20	0,006	0,99	1,18	21,28	0,63	4,87
2,0	0,99	21,92	21,35	0,02	0,99	0,57	15,67	0,70	2,34	0,96	20,70	20,15	0,009	0,99	0,66	12,59	0,87	5,51
Temp. (K)																		
291	0,97	27,17	25,00	0,002	0,99	1,54	6,59	0,93	20,00	0,97	45,04	43,20	0,001	0,98	2,02	17,38	0,98	13,15
298	0,99	45,66	43,00	0,002	0,99	2,27	16,92	0,91	11,63	0,95	35,08	34,20	0,006	0,99	1,18	21,28	0,64	4,87
308	0,99	37,73	36,50	0,002	0,99	1,63	15,61	0,98	13,70	0,98	44,64	43,90	0,005	0,99	1,13	30,53	0,93	4,56
Initial Con.(mg/L)																		
25	0,99	14,24	13,10	0,003	0,98	0,83	2,51	0,95	25,45	0,96	20,74	20,00	0,006	0,99	0,78	10,64	0,92	8,33
50	0,99	45,87	43,10	0,002	0,99	2,28	16,89	0,91	11,60	0,96	35,08	34,20	0,006	0,99	0,72	25,74	0,86	4,87
100	0,98	36,90	35,50	0,002	0,99	1,52	16,71	0,96	14,08	0,93	67,11	64,51	0,002	0,99	2,14	39,12	0,92	7,75
Initial pH																		
3,0	0,96	21,18	19,40	0,002	0,99	1,01	31,67	0,88	25,77	0,97	38,61	37,60	0,005	0,99	1,38	20,87	0,89	5,32
5,0	0,96	28,49	26,30	0,002	0,98	1,21	31,63	0,80	19,01	0,96	42,73	42,00	0,006	0,99	1,51	21,51	0,94	3,97
7,0	0,96	22,72	21,05	0,002	0,98	1,22	5,97	0,98	23,75	0,94	36,10	35,60	0,005	0,99	1,38	2,13	0,97	5,62
9,0	0,98	26,38	15,20	0,0009	0,85	0,86	24,59	0,94	73,10	0,94	28,49	26,17	0,002	0,97	1,46	8,13	0,94	9,11

Table 5: Thermodynamic parameters of OTC adsorption on different temperatures and adsorbents.

Adsorbents	T (K)	ΔG^0 (kJ/mol)	ΔH^0 (kJ/mol)	ΔS^0 (J/mol)	R^2
AC	291	-4,352	16,512	71,67	0,99
	298	-4,844			
	308	-5,570			
MagAC	291	-3,477	67,094	234,54	0,99
	298	-1,621			
	308	-5,006			
SBS/MagAC	291	-0,525	34,212	119,06	0,99
	298	-5,499			
	308	-2,547			
PC/MagAC	291	-4,473	43,598	157,80	0,95
	298	-2,439			
	308	-3,451			

Adsorption thermodynamics

Thermodynamic parameters of OTC adsorption on different temperatures and adsorbents are given in Table 5. ΔG^0 values Eq. (7) and the temperature range of 291-308K showing the spontaneous nature of the adsorption process. The negative values of ΔG^0 indicated the applicability of the sorption process and the positive values of ΔH^0 and ΔS^0 showed that the sorption process was endothermic in nature and had a random increase in the solid / liquid interface, respectively, during the sorption process. The positive ΔS value showed that the material has a good affinity with the dye molecules and there is an increase in the degree of freedom of the adsorbed species [63]. When the kinetic adsorption and thermodynamic results are examined, it is concluded that the physical adsorption in the polymer structure and the chemical interaction resulting from ion exchange of OTC molecules are involved in the adsorption event.

CONCLUSION

It was seen that AC, MagAC, SBS/MagAC and PC/MagAC can be good adsorbent materials to remove high OTC concentration in waste water and can be used for this purpose from the data obtained as a result of this study. Kinetic models showed that the adsorption process of OTC onto adsorbents at all temperatures conformed to so-called second-order and intra-particle diffusion patterns

rather than the so-called first-order kinetic model (R^2 : 0.99-1.00). In addition, the Langmuir isotherm model was found to be more suitable for OTC (R^2 : 0.98-1.00). It has been determined that polymer coated magnetic materials do not perform very well at high pH and all materials perform well at room temperature. Higher suitability was observed that AC, MagAC and PC/MagAC are more effective than SBS/MagAC to remove OTC. This situation was associated with the porosity of AC and other samples. It is seen that OTC can be removed from the aqueous environment more easily, especially when magnetic and polymeric materials are used to remove the adsorbent from the environment more easily.

Acknowledgements

This study was financially supported as a project (19/081/01/1/1) by Research Project Coordination Unit. Muğla Sıtkı Koçman University.

Received : Aug. 3, 2021 ; Accepted : Nov. 1, 2021

REFERENCES

- [1] Tran N.H., Reinhard M., Gin K.Y-H., [Occurrence and Fate of Emerging Contaminants in Municipal Wastewater Treatment Plants from Different Geographical Regions-A Review](#), *Water Res.*, **133**: 182–207 (2018).

- [2] Tien Duc P., Thi Thuy T., Van Anh L., Thu Thao P., Thi Huong D., Thanh Son L., Adsorption Characteristics of Molecular Oxytetracycline onto Alumina Particles: The Role of Surface Modification with an Anionic Surfactant, *J. Mol. Liq.*, **2871(8)**: 110- 900 (2019).
- [3] Cabello F.C., Heavy Use of Prophylactic Antibiotics in Aquaculture: A Growing Problem for Human and Animal Health and for the Environment, *Env. Microbiol.*, **8**: 1137-1144 (2006).
- [4] Jia L., Hua Z., Adsorption-Desorption of Oxytetracycline on Marine Sediments: Kinetics and Influencing Factors, *Chemosphere*, **164**:156-163 (2016).
- [5] Babaei A.A., Lima E.C., Takdastan A., Alavi N., Gholamreza G., Vosoughi M., Hassani G., Shirmardi M., Removal of Tetracycline Antibiotic from Contaminated Water Media by Multi-Walled Carbon Nanotubes: Operational Variables, Kinetics, and Equilibrium Studies, *Water Sci. Technol.*, **74**: 1202-1206 (2016).
- [6] Xiancai S., Dongfang L., Guowei Z., Matthew F., Xianrong M., Kexun L., Adsorption Mechanisms and the Effect of Oxytetracycline on Activated Sludge, *Bioresc Tech.*, **1512**: 428-431 (2014).
- [7] Jiayan W., Yanhua W., Zixuan W., Ya G., Xiaoping L., Adsorption Properties and Mechanism of Sepiolite Modified by Anionic and Cationic Surfactants on Oxytetracycline from Aqueous Solutions, *Sci. Total. Env.*, **708**: 134409 (2020).
- [8] Zhao C., Deng H., Li Y., Liu Z., Photodegradation of Oxytetracycline in Aqueous by 5A and 13X Loaded with TiO₂ under UV Irradiation, *J. Haz Mater.*, **176**: 884-892 (2010).
- [9] Wang C., Pan X., Fan Y., Chen Y., Mu W., The oxidative Stress Response of Oxytetracycline in the Ciliate Pseudocohnilembus Persalinus, *Env. Toxicol. Phar.*, **56**: 35-42 (2017).
- [10] Turku I., Sainio T., Paatero E., Thermodynamics of Tetracycline Adsorption on Silica, *Environ. Chem. Lett.*, **5**: 225-228 (2007).
- [11] Wang J.T., Hu J., Zhang S.W., Studies on the Sorption of Tetracycline onto Clays and Marine Sediment from Seawater, *J. Colloid Interface Sci.*, **349**: 578-582 (2010).
- [12] Cai W., Weng X., Chen Z., Highly Efficient Removal of Antibiotic Rifampicin from Aqueous Solution Using Green Synthesis of Recyclable Nano-Fe₃O₄, *Environ Pollut.*, **247**: 839–846 (2019).
- [13] Asfaram A., Ghaedi M., Goudarzi A., Rajabi M., Response Surface Methodology Approach for Optimization of Simultaneous Dye and Metal Ion Ultrasound-Assisted Adsorption onto Mn Doped Fe₃O₄-NPs Loaded on AC: Kinetic and Isothermal Studies, *Dalton Transactions*, **33**: (2015).
- [14] Shaker M.A., Yakout A.A., Optimization. Isotherm. Kinetic and Thermodynamic Studies of Pb(II) Ions Adsorption onto N-Maleated Chitosan-Immobilized TiO₂ Nanoparticles from Aqueous Media, *Spec. Acta. Part A.*, **154**: 145-156 (2016).
- [15] Ghaedi M., Khafri H.Z., Asfaram A., Goudarzi A., Response Surface Methodology Approach for Optimization of Adsorption of Janus Green B from Aqueous Solution onto ZnO/Zn(OH)₂-NP-AC: Kinetic and Isotherm Study, *Spectrochim Acta. Part A.*, **152**: 233-240 (2016).
- [16] Davarnejad R., Panahi P., Cu (II) Removal from Aqueous Wastewaters by Adsorption on the Modified Henna with Fe₃O₄ Nanoparticles Using Response Surface Methodology, *Sep. Purif. Technol.*, **158**: 286-292 (2016).
- [17] Akin D., Yakar A., Gunduz U., Synthesis of Magnetic Fe₃O₄-Chitosan Nanoparticles by Ionic Gelation and their Dye Removal Ability, *Water Environ. Res.*, **87**: 425-436 (2015).
- [18] Bagheri A.R., Ghaedi M., Asfaram A., Bazrafshan A.A., Jannesar R., Comparative Study on Ultrasonic Assisted Adsorption of Dyes From Single System onto Fe₃O₄ Magnetite Nanoparticles Loaded on Activated Carbon: Experimental Design Methodology, *Ultra Sonic.*, **34**: 294-304 (2017).
- [19] Bhatia D., Datta D., Joshi A., Gupta S., Gote Y., Adsorption Study for the Separation of Isonicotinic Acid from Aqueous Solution Using Activated Carbon/Fe₃O₄ Composites, *J. Chem. Eng. Data.*, **63**: 436-445 (2018).
- [20] Zhang S., Wang Z., Chen H., Kai C., Jiang M., Wang Q., Zhou Z., Polyethylenimine Functionalized Fe₃O₄/Steam-Exploded Rice Straw Composite as An Efficient Adsorbent for Cr(VI) Removal, *Appl. Surf. Sci.*, **440**: 1277-1285 (2018).

- [21] Badi M.Y., Azari A., Pasalari H., Esrafilı A., Farzadkia M., [Modification of Activated Carbon with Magnetic Fe₃O₄ Nanoparticle Composite for Removal of Ceftriaxone from Aquatic Solutions](#), *J. Mol. Liq.*, **261**: 146-154 (2018).
- [22] Wen T., Wang J., Yu S., Chen Z., Hayat T., Wang X., [Magnetic Porous Carbonaceous Material Produced from Tea Waste for Efficient Removal of As\(V\), Cr\(VI\), Humic Acid, and Dyes](#), *ACS Sustain. Chem. Eng.*, **5**: 4371-4380 (2017).
- [23] Angelia E., Seyfferth L., Richard S.F., Luthy G., [Immobilization of Hg\(II\) in Water With Polysulfide-Rubber \(PSR\) Polymer-Coated Activated Carbon](#), *Wat Res.*, **45**(2): 453-460 (2011).
- [24] Yang N., Zhu S., Zhang D., Xu S., [Synthesis and Properties of Magnetic Fe₃O₄-Activated Carbon Nanocomposite Particles for Dye Removal](#), *Mat. Letters*, **62**(4-5): 645-650 (2008).
- [25] Kakavandi B., Jafari A.J., Kalantary R.R., Nasserı S., Ameri A., Esrafilı A., [Synthesis and Properties of Fe₃O₄-Activated Carbon Magnetic Nanoparticles for Removal of Aniline from Aqueous Solution: Equilibrium, Kinetic and Thermodynamic Studies](#), *Iran. J. Env. Health Sci. & Eng.*, **10**(1): 19 (2013).
- [26] Fard M.A., Vosoogh A., Aminzadeh B., [Using Polymer Coated Nanoparticles for Adsorption of Micropollutants from Water](#), *Colloids and Surfaces A: Physicochemical and Engineering Aspects*, **531**: 189-197 (2017).
- [27] Lagergren S., [About the theory of So-Called Adsorption of Soluble Substances](#), *Sven Vetenskapsakad Handlingar*, **24**: 1-39 (1898).
- [28] Ho Y.S., McKay G., [Pseudo-Second order Model for Sorption Processes](#), *Proc. Biochem.*, **34**: 451-465 (1999).
- [29] Acemioglu B., [Batch Kinetic Study of Sorption of Methylene Blue by Perlite](#), *Chem. Eng. J.*, **106**(1): 73-81 (2005).
- [30] Uğurlu M., [Kinetic of the Adsorption of Reactive Dyes by Using Sepiolite Mineral](#), *Mic. and Mes. Mat.*, **119**: 276-283 (2009).
- [31] Uğurlu M., Karaoğlu M.H., [Adsorption Studies and Removal of Ammonium from Bleached Kraft Mill Effluent by Fly Ash and Sepiolite](#), *Mic. and Meso. Mate.*, **139**(1-3): 173-178 (2011).
- [32] Girgis B., Temerk Y., Gadelrab M.M., Abdullah I., [X-Ray Diffraction Patterns of Activated Carbons Prepared Under Various Conditions](#), *Car Letters*, **8**(2): 95-100 (2007).
- [33] Vaizoğullar A.İ., [TiO₂/ZnO Supported on Sepiolite: Preparation, Structural Characterization, and Photocatalytic Degradation of Flumequine Antibiotic in Aqueous Solution](#), *Chem. Eng. Com.*, **204**(6): 689-697 (2017).
- [34] Oliveiraa G.F.D., Andradeb R.C.D., Trindadea M.A.G., Andradeb H.M.C., Carvalhoa C.T.D., [Thermogravimetric and Spectroscopic Study \(tg-dta/ft-ir\) of Activated Carbon from the Renewable Biomass Source Babassu](#), *Quim. Nova.*, **40**(3): 284-292 (2017).
- [35] Uğurlu M., Gürses A., Açıkyıldız M., [Comparison of Textile Dyeing Effluent Adsorption on Commercial Activated Carbon and Activated Carbon Prepared from Olive Stone by ZnCl₂ Activation](#), *Micro and Meso Mate*, **111**: 228-235 (2008).
- [36] Uğurlu M., Yılmaz S.İ., Vaizoğullar A.İ., [Removal of Color and COD from Olive Wastewater by Using Three-Phase Three-Dimensional \(3D\) Electrode Reactor](#), *Mat. Today: Proce.*, **18**: 1986-1995 (2019).
- [37] Mazloomi F., Jalali M., [Ammonium Removal from Aqueous Solutions by Natural Iranian Zeolite in the Presence of Organic Acids, Cations and Anions](#), *J. Env. Chem. Eng.*, **4**: 1664-1673 (2016).
- [38] Lin Y., Xu S., Li J., [Fast and Highly Efficient Tetracyclines Removal from Environmental Waters by Graphene Oxide Functionalized Magnetic Particles](#), *Chem. Eng. J.*, **225**: 679-685 (2013).
- [39] Jia M., Wang F., Bian Y., Jin X., Song Y., Kengara F.O., Xu R., Jiang X., [Effects of pH and Metal Ions on Oxytetracycline Sorption to Maize-Straw-Derived Biochar](#), *Biores. Technol.*, **136**: 87-93 (2013).
- [40] Abbott T., Bıcakcı G.K, Mohammad S.I, Eskicioglu Ç., [A Review on the Fate of Legacy and Alternative Antimicrobials and their Metabolites During Wastewater and Sludge Treatment](#), *Int. J. Mol. Sci.*, **21**(23): 9241 (2020).
- [41] Liao P., Zhan Z., Dai J., Wu X., Zhang W., Wang K., Yuan S., [Adsorption of Tetracycline and Chloramphenicol in Aqueous Solutions by Bamboo Charcoal: A Batch and Fixed-Bed Column Study](#), *Chem. Eng. J.*, **228**: 496-505 (2013).

- [42] Bağda E., Erşan M., Bağda E., Investigation of Adsorptive Removal of Tetracycline with Sponge Like, Rosa Canina Gall Extract Modified, Polyacrylamide Cryogels, *J. Environ. Chem. Eng.*, **1**: 1079–1084 (2013).
- [43] Eniola J.O., Kumar R., Barakat M.A., Adsorptive Removal of Antibiotics from Water over Natural and Modified Adsorbents, *Environ. Sci. Pollut. Res.*, **26**: 34775–34788 (2019).
- [44] Wang Z., Yang X., Qin T., Liang G., Li Y., Xie X., Efficient Removal of Oxytetracycline from Aqueous Solution by a Novel Magnetic Clay–Biochar Composite Using Natural Attapulgite and Cauliflower Leaves, *Environ. Sci. Pollut. Res. Int.*, **26**: 7463–7475 (2019).
- [45] Wu J., Wang Y., Wu Z., Gao Y., Li X., Adsorption Properties and Mechanism of Sepiolite Modified by Anionic and Cationic Surfactants on Oxytetracycline from Aqueous Solutions, *Sci. of Total. Env.*, **708**: 13440 (2020).
- [46] Johnston A-L., Lester, E., Williams O., Gomes R.L., Understanding Layered Double Hydroxide Properties as Sorbent Materials for Removing Organic Pollutants from Environmental Waters, *J. Env. Chem. Eng.*, **9**(4): 105197 (2021)
- [47] Eniola J.O., Kumar R., Mohamed O.A., Al-Rashdi A.A., Barakat M.A., Synthesis and Characterization of CuFe₂O₄/NiMgAl-LDH Composite for the Efficient Removal of Oxytetracycline Antibiotic, *J. of S. Chem. Soci.*, **23**: 139-150 (2019).
- [48] Liu X., Zhang H., Luo Y., Zhu R., Wang H., Huang B., Sorption of OTC in Particulate Organic Matter Soils and Sediments: Roles of pH, Ionic Strength and Temperature, *Sci. of the Total.*, **714**: 13662 (2020).
- [49] Qin Q., Wu X., Chen L., Jiang Z., Xu Y., Simultaneous Removal of Tetracycline and Cu(II) by Adsorption and Coadsorption Using Oxidized Activated Carbon, *RSC Adv.*, **8**(4): 1744–1752 (2018).
- [50] Chang P., Jean J., Jiang W., Li Z., Mechanism of Tetracycline Sorption on Hectorite, *Colloids Surf. A Physicochem. Eng. Asp.*, **339**: (1) 94–99 (2009).
- [51] Jutta R.V.P., David A.L., Sorption of Tetracycline and Chlorotetracycline on K- and Ca-saturated Soil Clays, Humic Substances, and Clay-Humic Complexes. *Env. Sci. & Tech.*, **41**(6): 1928–1933 (2007).
- [52] Wang S., Hui H., Adsorption Behavior of Antibiotic in Soil Environment: A Critical Review, *Front. Environ. Sci. Eng.*, **9**: 565-574 (2015).
- [53] Sassman S.A., Lee L.S., Sorption of Three Tetracyclines by Several Soils: Assessing the Role of pH and Cation Exchange, *Env. Sci. & Tech.*, **39**(19): 7452–7459 (2005).
- [54] Sun Y., Yue Q., Gao B., Li Q., Huang L., Yao F., Xu X., Preparation of Activated Carbon Derived from Cotton Linter Fibers by Fused NaOH Activation and its Application for Oxytetracycline (OTC) Adsorption, *J. Colloid. and Interface Sci.*, **368**: 521-52 (2012).
- [55] Lii J., Zhang H., Adsorption- Desorption of Oxytetracycline on Marine Sediments: Kinetic and Influencing Factors, *Chemosphere*, **164**: 156-163 (2016).
- [56] Kan Y., Yue Q., Li D., Wu Y., Gao B., Preparation and Characterization of Activated Carbons from Wastewater by H₃PO₄ Activation in Different Atmospheres for Oxytetracycline Removal, *J.T. Ins. Chem. Eng.*, **71**: 494-500 (2017)
- [57] Li R., Liang N., Ma X., Chen B., Huang F., Study on the Adsorption Behavior of Glycerin from Fatty Acid Methyl Esters by a Tertiary Amine-Type Anion Exchange Resin, *J. Chrom. A.*, **1586**: 62-71 (2019).
- [58] He X., Wang B., Zhang Q., Phenols Removal from Water by Precursor Preparation for MgAl Layered Double Hydroxide: Isotherm. Kinetic and Mechanism, *Mater. Chem. Phys.* **221**: 108-117 (2019).
- [59] Li N., Zhou L., Jin X., Owens G., Chen Z., Simultaneous Removal of Tetracycline and Oxytetracycline Antibiotics from Wastewater Using a ZIF-8 Metal Organic-Framework, *J. Hazard Mat.*, **366**: 563–57 (2019).
- [60] Eniola J.O., Kumar R., Al-Rashdi A.A., Ansari M.O., Barakat M.A., Fabrication of Novel Al(OH)₃/CuMnAl-Layered Double Hydroxide for Detoxification of Organic Contaminants from Aqueous Solution, *ACS Omega*, **4**(19): 18268-18278 (2019).
- [61] Ji L., Chen W., Duan L., Zhu D., Mechanisms for Strong Adsorption of Tetracycline to Carbon Nanotubes: A Comparative Study Using Activated Carbon and Graphite as Adsorbents. *Env. Sci. & Tech.*, **43**(7): 2322-2327 (2009).

- [62] Belaib F., Azzedine M., Boubeker B., Abdeslam-Hassen M., [Experimental Study of OTC Retention by Adsorption onto Polyaniline Coated Peanut Shells](#), *I. J. Hydrogen Energy*, **39**: 1511-1515 (2014).
- [63] Renault F., Morin-Crini N., Gimbert F., Badot P., Crini G., [Cationized Starch-Based Material as a New Ion-Exchanger Adsorbent for the Removal of C.I. Acid Blue 25 from Aqueous Solutions](#), *Biores. Tech.*, **99**: 7573-7586 (2008).